Figure S1 Temperature-controlled stage and lid warmer.

Colors indicate independent experiments. (**A**) Stage temperature was set to 29.5 ºC and was maintained at within 1ºC of the set temperature except for the initial period of time. Growth rates at 5 µM (as seen in Figure 4) for all three experiments were similar (0.50 +/- 0.02/hr) despite the observed ~0.5ºC differences in temperature. (**B**) The lid warmer maintained the microplate lid 0.5~ 0.8ºC above the stage temperature. The average temperature difference was 0.68ºC. A LabVIEW program compared temperature readings from the stage and from the lid warmer, and turned on and off the heater to maintain the set range of temperature difference.

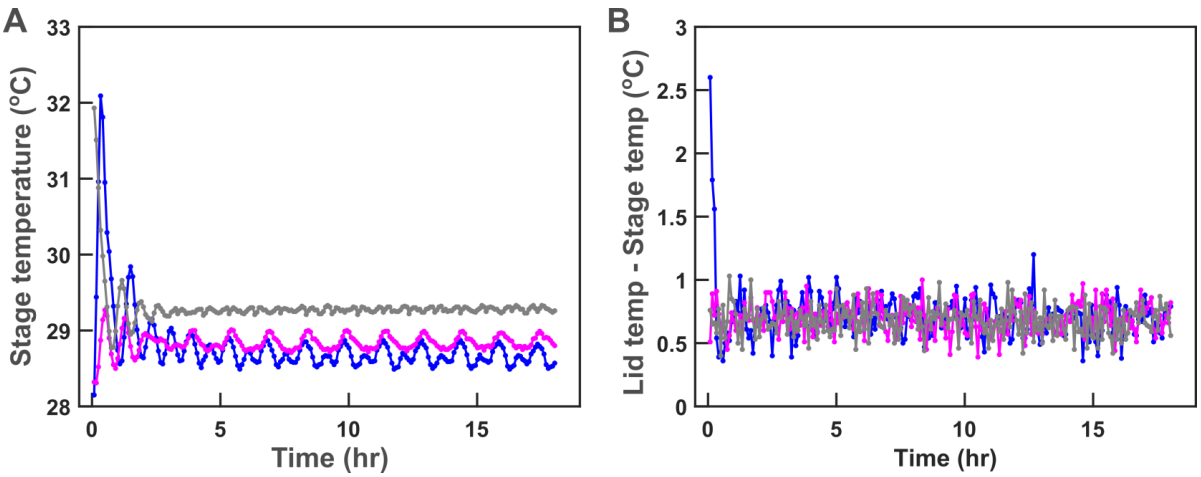

Figure S2 Well location does not significantly impact growth rate.

To examine potential well-position bias in growth rate, we quantified growth rates of *lys2-* cells across various wells of a 96-well plate at an identical initial lysine concentration. **(A)** We did not observe any correlation between well position and growth rate at 10 µM (non-limiting) lysine in either of the two experiments (left and right). **(B)** There was a slight correlation between well position and growth rate at 2.5 µM (limiting) lysine. Wells that supported faster growth in one experiment tended to support faster growth in the other (left vs right). Possible causes could be the order in which cells were imaged or small systematic differences in temperature. Since the variation was still within a reasonable range (+/- 0.04 /hr, see **C**), we did not investigate this further. **(C)** Growth rates averaged across wells in a plate were similar between two independent experiments. Error bars represent 2*standard deviations.

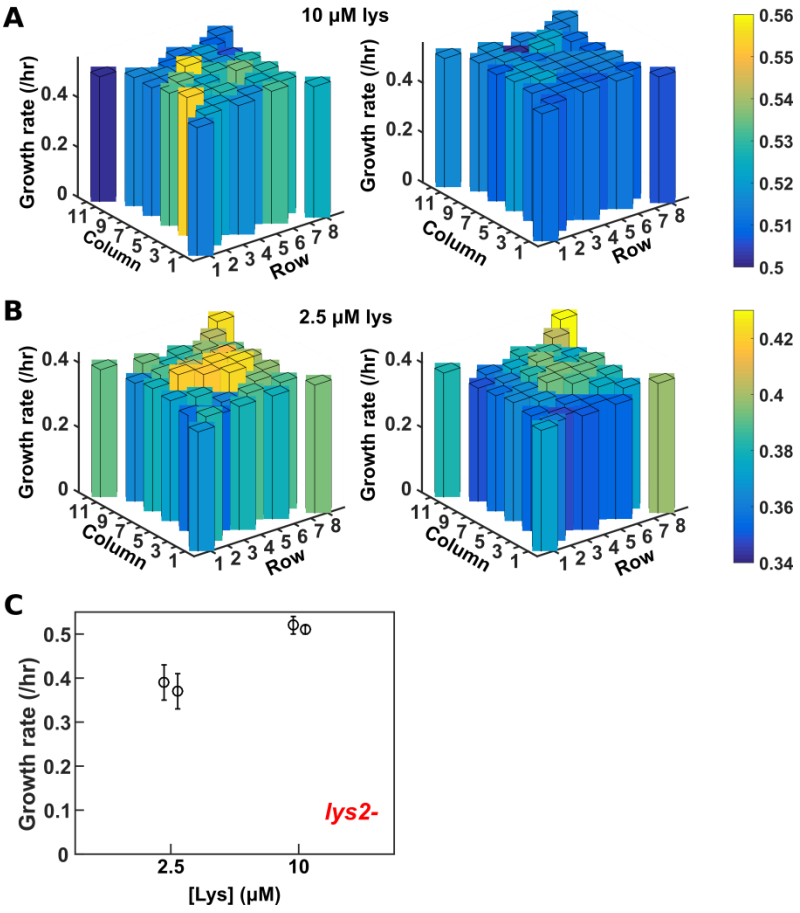

Figure S3 A linear relationship between total live cell density and total fluorescence intensity in a field of view.

Various numbers of live cells (counted by flow cytometry) were placed in minimal medium lacking glucose (to arrest cell growth) in microtiter wells and allowed to settle to the bottom of wells. The plate was then imaged using our microscope setup to measure the total fluorescence intensity. For both red (mCherry-expressing *lys2*-) and green (GFP-expressing *ade8*-) fluorescent strains, total live cell densities and total background-subtracted fluorescence intensities in a field of view displayed linear relationships. At the highest density, there were at least nine cell layers.

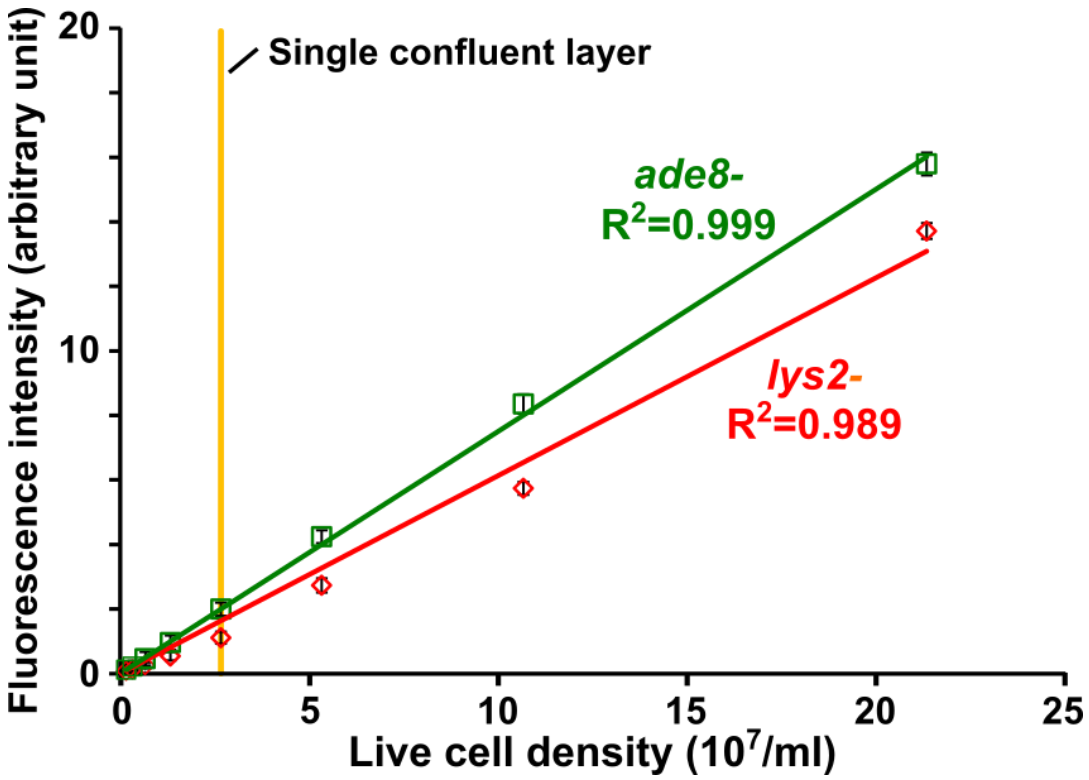

Figure S4 Microscopy and flow cytometry measurements reveal multi-phasic death dynamics of lys2- cells.

We grew *lys2-* (WY1335) in excess lysine. At time zero, we washed cells free of lysine, and pre-starved cells for 4~5 hrs to deplete vacuolar lysine storage. We then diluted cells in SD (<20,000 cell/ml) and imaged them. (**A**) Microscopy total fluorescence intensity (circles) and flow cytometry (diamonds) revealed multi-phasic death kinetics (slow death rate followed by faster death rate). We also periodically concentrated cells from a fraction of wells for flow cytometry measurements. Error bars are 2x standard deviations from multiple independent measurements (three technical replicates for FACS, and four images for fluorescence imaging). (**B**) Cell counts (diamonds) and total fluorescence intensity (circles) revealed multi-phasic death kinetics. Total fluorescence intensity and live cell counts (~200 cells) in two positions were followed over time. In both panels, different colors represent experiments done on different days.

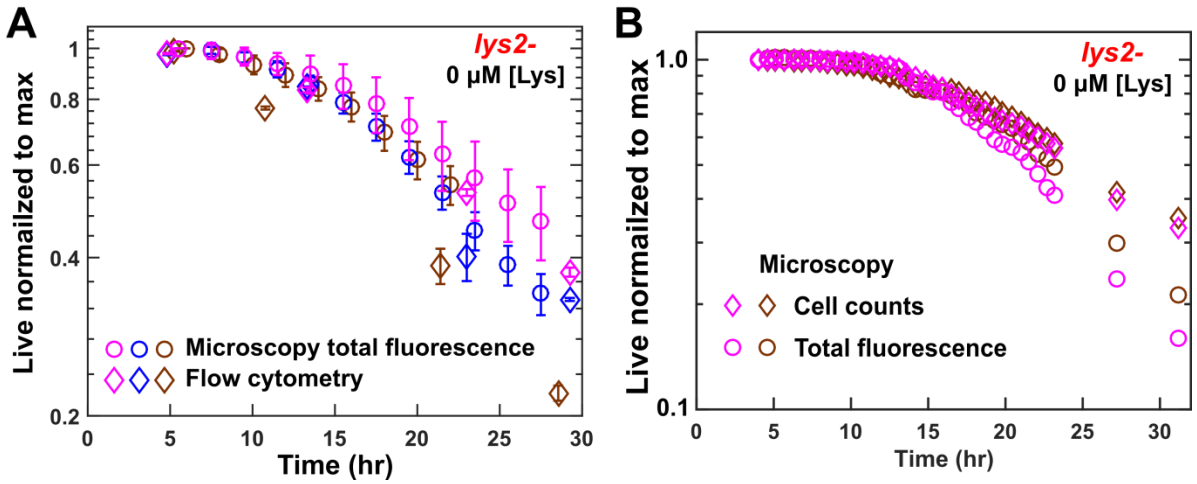

Figure S5 A comparison of CellQuant and manual counts.

lys2- was washed, pre-starved for four hours, and then imaged at 0 μM lysine every hour for 24 hours. Four separate positions were imaged over time, and images were analyzed by manual and automated CellQuant counting (Methods, "Individual cell tracking at low metabolite concentrations") and results were compared. **(A)** CellQuant counts correlate with manual counts (R^2 = 0.9455), though CellQuant counts were 90% that of manual counts. **(B)** Death rates calculated from manual and CellQuant counts over the 6-24hr starvation time window of the assay by aggregating the four separate image cell counts. Error bars are 2*fitting error of the regression.

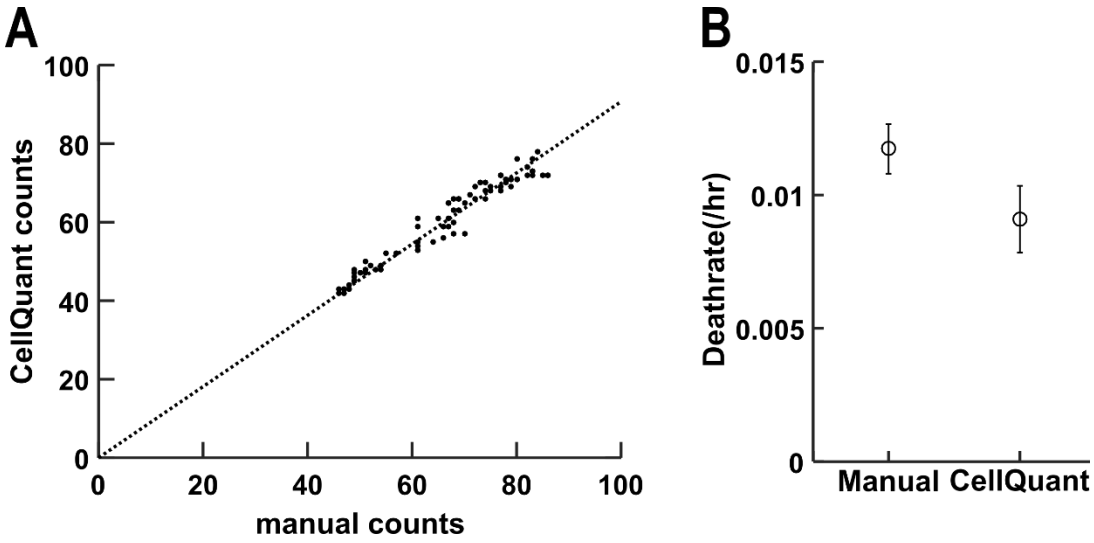

Figure S6 Low concentrations of required metabolite supported birth for ade8- but not lys2- cells.

(**A**) *lys2*- cells grown in excess lysine were washed free of lysine at time zero, and birth events over the preceding 1-hr interval were counted at various times. Data source was identical to that in Figure 2A. (**B**) We grew *ade8*- cells in excess hypoxanthine to exponential phase, washed away hypoxanthine, and prestarved cells for 24 hrs. At time zero, we started imaging. Birth events over the preceding 2-hr interval were counted at various times. Data source was identical to that in Figure 3C.

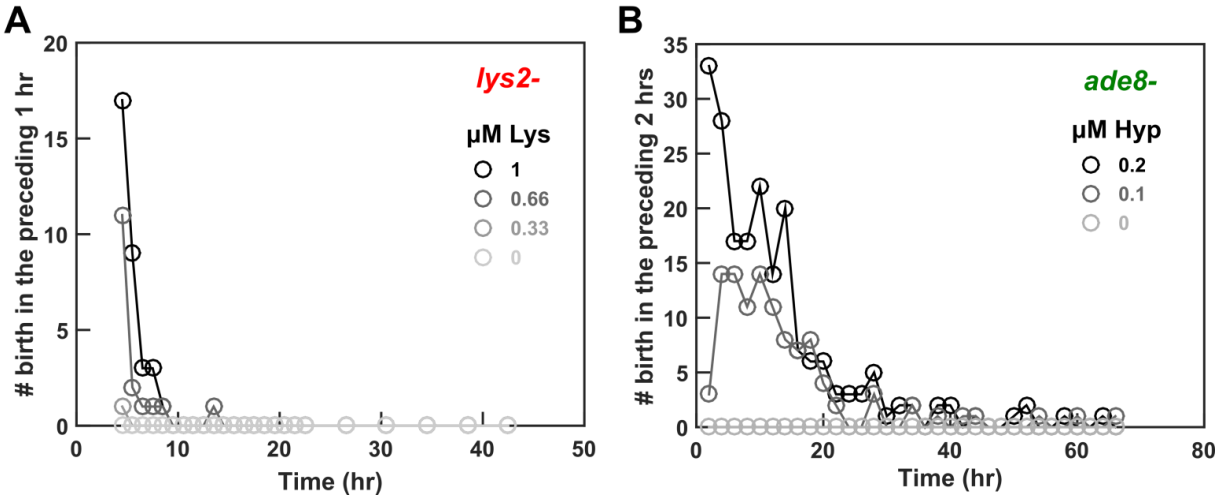

Figure S7 An increase in fluorescence intensity may not correspond to cell birth.

We imaged *lys2-* cells (161 total) in 0.33 µM lysine. Total fluorescence intensity (brown) and counts of fluorescent cells (blue) over time were plotted. We observed no birth events in this experiment, while fluorescence increased for over 15 hours after the start of the experiment.

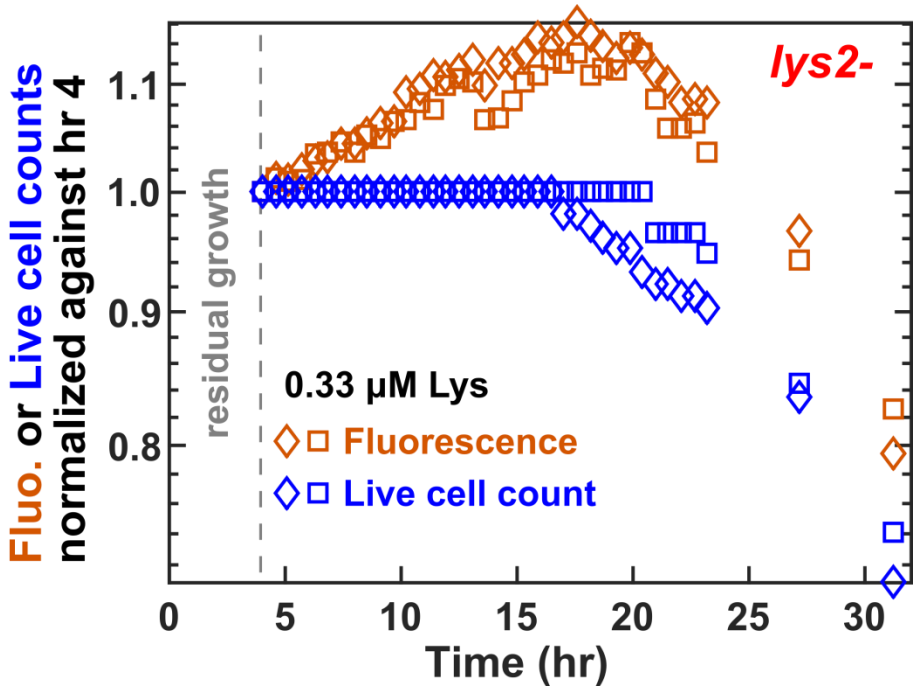

Figure S8 Steady growth rate is maintained only for ≥2.5 µM lysine.

We calculated growth rates from fluorescence intensity over time. Each data point corresponded to the growth rate calculated over the four previous time points, a time window of approximately 1.7 hours. For ≥2.5 µM lysine, cells reached a maximal growth rate and maintained it across at least two sliding windows (e.g. hours ~5-8 for 3.75 and 5 µM). For 1.75 µM lysine, the growth rate declined throughout the duration of measurements. For ≤1 µM lysine, any positive growth rate after residual growth was due to cell swelling not cell birth (Supp Fig 5).

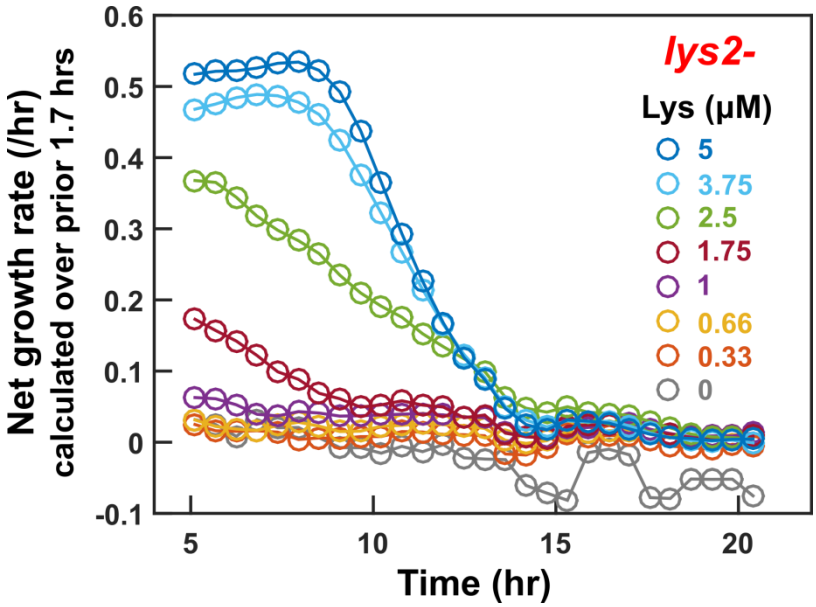

Figure S9 Chemostat dynamics rapidly reach a steady state.

lys2- cells growing exponentially in excess lysine were washed free of lysine, and inoculated in a chemostat vessel at 1/3 steady-state density in the presence of ~10-15 µM lysine. Minimal medium containing 20 µM lysine was dripped into the culturing vessel (19 ml) at a set rate to achieve the desired growth rate (8-hr doubling time corresponding to a dilution rate of ln(2)/8=0.0866/hr and a flow rate of 19 ml*ln(2)/8 hr = 1.646 ml/hr; "Chemostat culturing" in Methods). We tracked live and dead cell densities **(A)** using flow cytometry (Methods, "Flow cytometry") and tracked lysine concentrations **(B)** using a bioassay (Methods, "Bioassay").

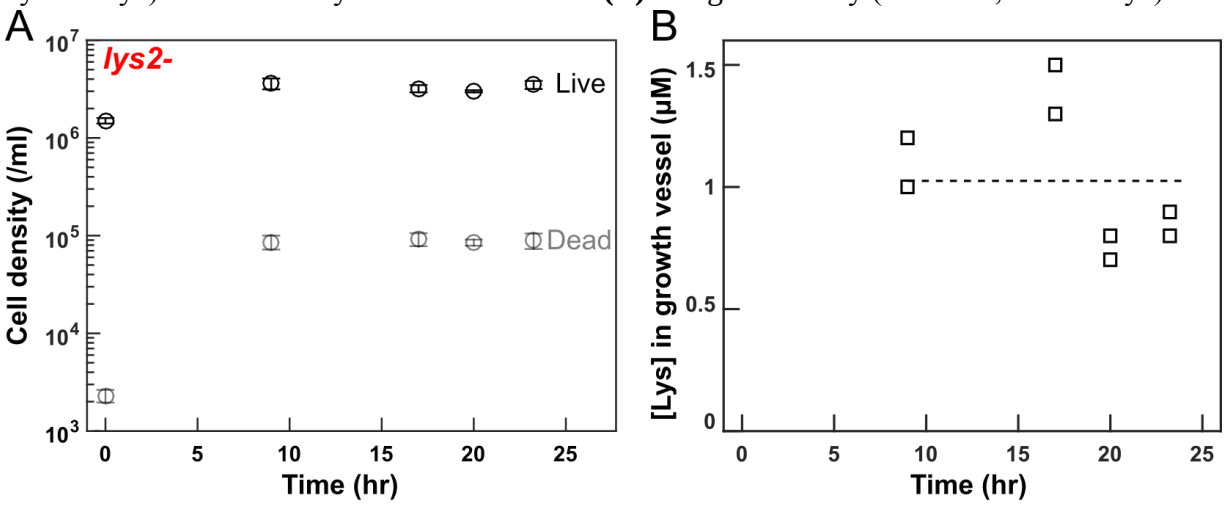

Figure S10 Birth rates of ade8- as a function of hypoxanthine concentrations.

ade8- (WY1340) cells were grown to exponential phase in minimal medium supplemented with excess hypoxanthine, washed free of hypoxanthine, and pre-starved for 24 hrs to deplete cellular storage. Cells were then incubated at various concentrations of hypoxanthine and imaged. The Monod model (grey dotted line) predicted a maximal birth rate of 0.49/hr (95% CI: 0.46~ 0.52/hr). In the Moser model (black), maximal birth rate $b_{\max} = 0.44$/hr (95% CI: 0.43 ~ 0.45), hypoxanthine concentration for half maximal birth rate $K_m = 1.3$ μM (95% CI: 1.2 ~ 1.4), and $n = 1.5$ (95% CI: 1.4~ 1.7). In comparison, experimentally-measured b_{max} was 0.44 ± 0.03/hr.

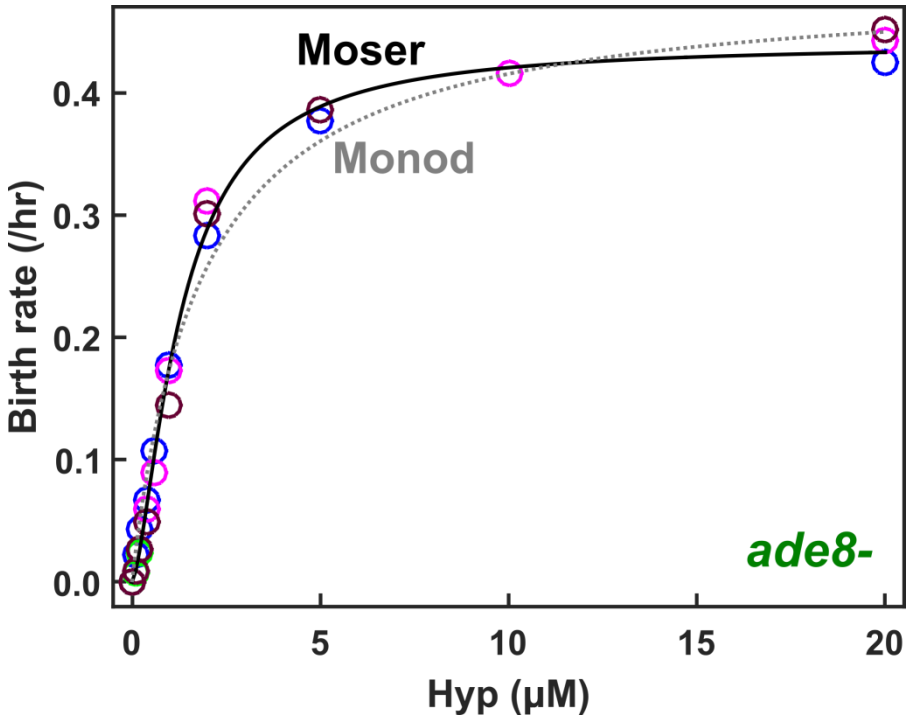

Figure S11 The duration of pre-starvation can affect growth rates.

lys2- cells were grown to exponential phase in excess lysine. At time zero, we washed cells free of lysine, and pre-starved them for 0, 3, or 6 hrs to deplete cellular lysine storage before imaging them in various concentrations of lysine. We analyzed data from hour 3 and on (post-residual growth). Using 3-hr sliding time windows, we calculated the growth rate over time. We plotted maximal growth rate with error bars indicating 2x error of slope estimation. Note that in 0~1μM lysine, we used fluorescence to quantify growth rate and did not correct for the absence of birth, and hence the perceived positive growth rates.

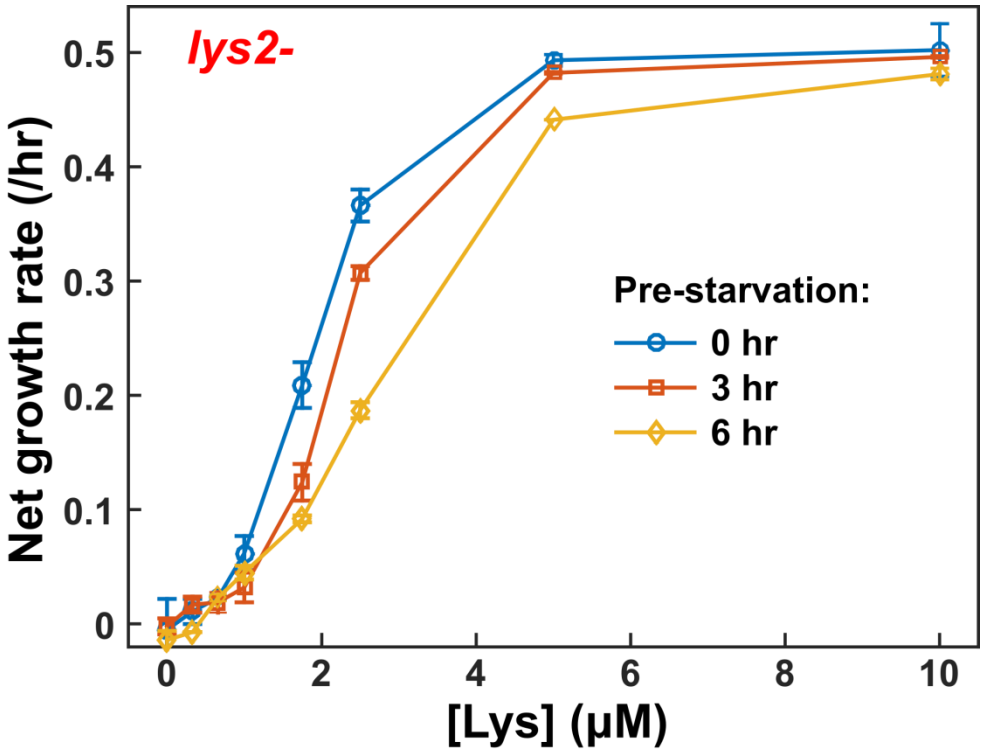

Figure S12 Autofocusing.

Adequate fluorescence images can be obtained by choosing the local minimum of the autofocus score as our imaging plane. **(A)** The autofocus score *A(z)* had two local maxima (i and iii), corresponding to image artifacts created by lensing effects of yeast cells (see **D** and **E** for a qualitative explanation). Bright-field **(B)** and fluorescence **(C)** images were taken near z = -24 μm (i), 0 μm (ii), and 14 μm (iii), corresponding to local maximum, local minimum, and local maximum *A(z)*, respectively. It is apparent from (**B**) that positions i and iii had large contrast and thus large *A(z)*. Fluorescence images taken at positions ii and iii were more in focus than that at position i. Position ii was used for fluorescence imaging. **(D, E)** A qualitative explanation of autofocusing. The density of light rays in a given *z* plane corresponds to the apparent brightness. **(D)** When position iii is in the focal plane of the camera, real light rays (blue) have been focused by the cell (yellow) to generate an image of a bright spot (which looks bigger than a point due to diffraction) with a dark ring (corresponding to iii in **B**). At position ii, light intensities inside and outside of the cell are similar (corresponding to ii in **B**). **(E)** At position i, the virtual rays (red) create the image of a bright hallow around a dark center.

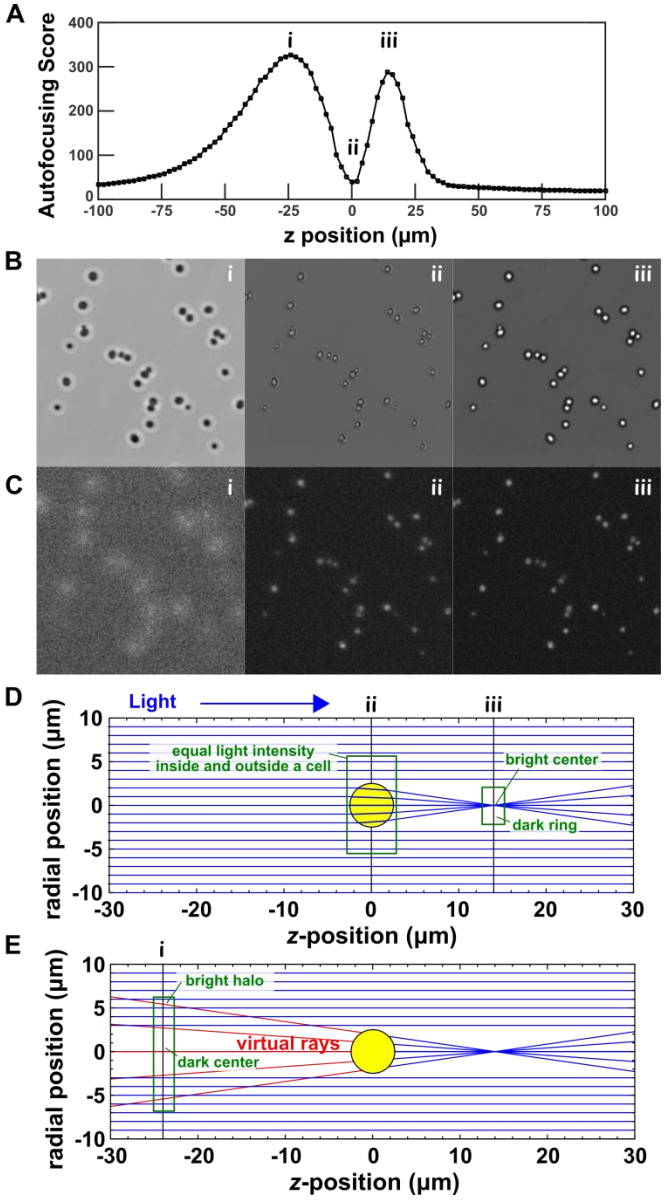

Figure S13 Intermediate images used for CellQuant analysis

(A) CellQuant takes as input bright-field images that are out of focus such that cells appear white surrounded by a dark ring. (**B**) After identifying the average background value I_A in **A**, the intensity of each pixel was adjusted in the following manner: intensity values $\geq I_A$ were assigned white (255 in an 8-bit image), and intensity values $\in[0\ I_A]$ were re-scaled to [0 255]. This caused cells to appear as dark rings in a bright background. (**C**) Cell selections were made using ImageJ's "Find Maxima..." and "Analyze Particles..." algorithms. Cell selections were then applied on the original bright-field image to distinguish real cells (which have high variance in intensity) to spurious background selections (which have low variance in intensity). Next, cell selections were applied to their corresponding background-subtracted fluorescence image (**D**) to determine the fluorescence intensity of each cell. Cells with mean fluorescence less than 1.0 SD above the mean background were considered to be dead.

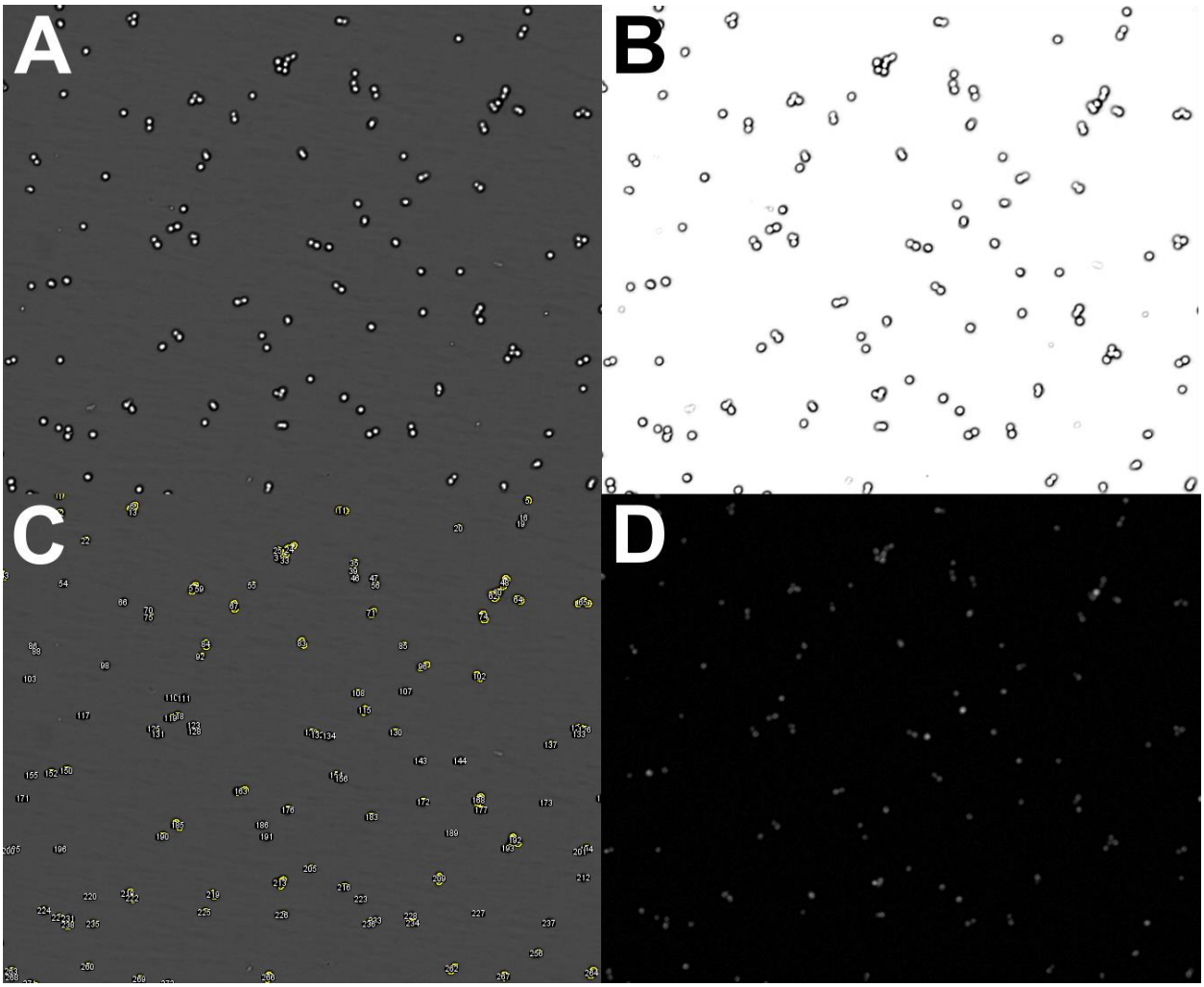

Figure S14 Bioact image analysis.

Bioact creates a mask that defines the regions of the image that contain cells. The first **(A)** and last **(B)** fluorescent images from a growth experiment show the cells, together with their background. Masks for the first and last images created by Bioact are shown in **(C)** and **(D),** with the cell-containing foreground in white and the background in black. These masks were applied to the original image when calculating foreground fluorescence intensity.

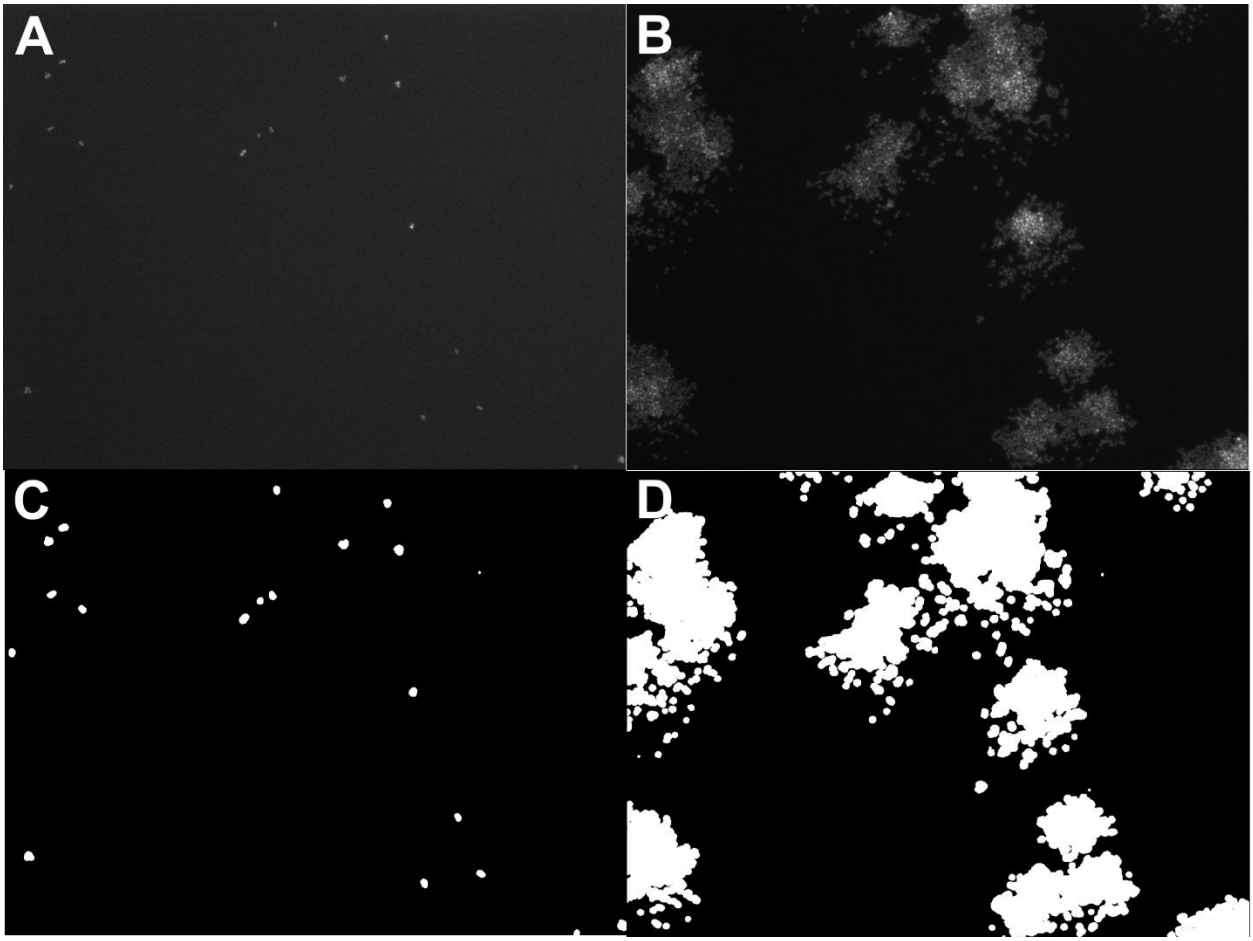

Figure S15 Using an evolved clone to measure low concentrations of lysine.

WY2270, an evolved *lys2*- clone with significantly improved affinity for lysine compared to WY1335, can detect lysine as low as 0.1 µM. Dotted line marks detection limit. Circles and diamonds mark two independent replicates.

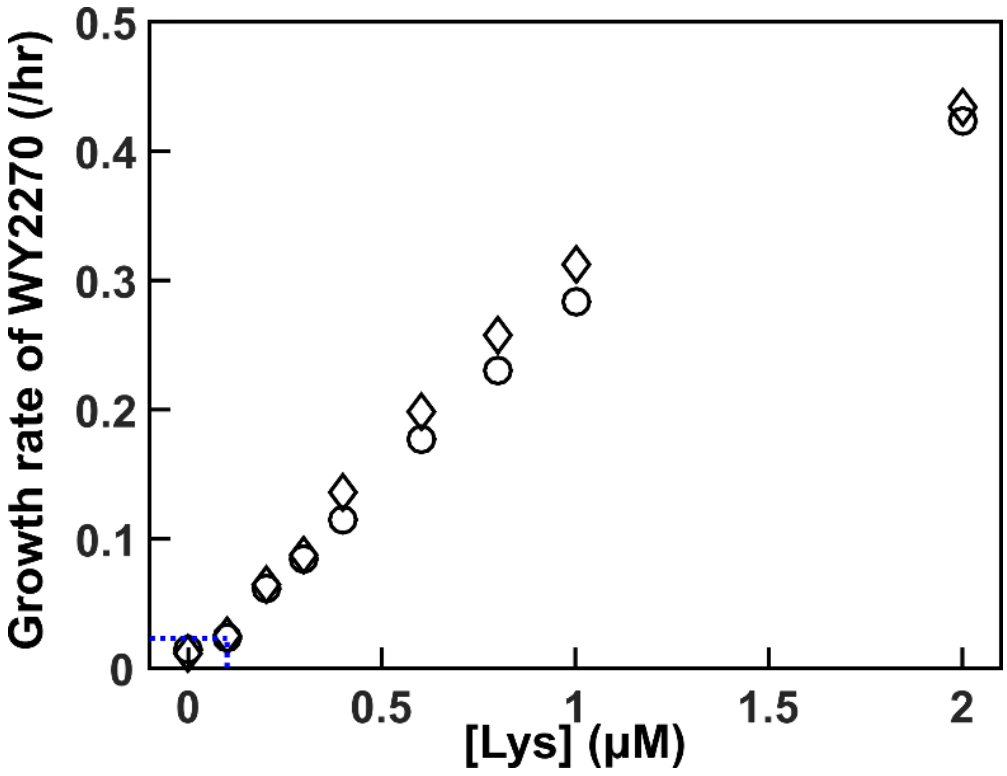

Supplementary Movie 1 Time-lapse fluorescence microscopy of lys2- at high lysine.

Supplementary Movie 2 Time-lapse fluorescence microscopy of lys2- at low (0.66 µM) lysine.

Supplementary Movie 3 Time-lapse fluorescence microscopy of lys2- at zero lysine.

Supplementary Movie 4 ade8- cell re-dividing after having transiently lost fluorescence.

Supplementary Movie 5 Time-lapse bright-field microscopy of lys2- at zero lysine.